Arabian Journal of Chemistry (2015) xxx, xxx–xxx

King Saud University

Arabian Journal of Chemistry

www.ksu.edu.sa
www.sciencedirect.com

ORIGINAL ARTICLE

Simple one-pot sonochemical synthesis of copper sulphide nanoparticles for solar cell applications

Alok Singh [a], R. Manivannan [b], S. Noyel Victoria [a,*]

[a] Department of Chemical Engineering, National Institute of Technology Karnataka, Surathkal, Karnataka 575025, India
[b] Department of Chemical Engineering, National Institute of Technology Raipur, Chhattisgarh 492010, India

Received 26 November 2014; accepted 21 March 2015

KEYWORDS

Sonication;
Copper sulphides;
Nanoparticles;
XRD;
SEM;
TEM

Abstract Copper sulphide nanoparticles for solar cell applications were synthesized by a single step sonochemical method using copper acetate and thiourea as precursors. The effects of sonication time, ultrasonic bath temperature and annealing temperature on particle properties were studied. Synthesized particles were characterized using scanning electron microscope, transmission electron microscope, X-ray diffraction spectrophotometer and UV–visible spectrophotometer. The particles were found to be a mixture of chalcocite, covellite and djurleite. The optical band gap of the particles was found to be in the range of 1.6–2.1 eV. Heat treatment of the particles was found to give rise to needle shaped particles while a bath temperature of 55 °C yielded few nanoplates.

1. Introduction

In recent times the synthesis of metal chalcogenide nanoparticles has gained importance because of their unique properties at the nanoscale when compared to their bulk counterparts. Such unique properties of the semiconductor nanoparticles make them an ideal candidate for photovoltaic applications (Kassim et al., 2010). Of the semiconducting materials, their metal sulphides are studied in abundance because of their characteristic band gap, high extinction coefficient which makes them an ideal candidate for solar cells applications as light absorbers (Saraf, 2012). Simplest among the semiconductor metal chalcogenides are copper sulphides which fall in the binary semiconductor category. The Cu_xS, which is a P-type semiconductor with the copper vacancies as acceptor sites with x taking values between 1 and 2, Cu_2S (chalcocite), CuS (covellite), $Cu_{1.96}S$ (djurlite), $Cu_{1.8}S$ (digenite), $Cu_{1.75}S$ (anilite) are more common (Zhao et al., 2009, 2010). The optical properties of Cu_xS greatly depend on the copper vacancies (Zhao et al., 2009). The Cu_xS have varying band gap depending on the value of x, for instance, E_{gind} is 1.05 eV and E_{gdir} is 1.7 eV when x takes the value 2 which is for Cu_2S (Chalcocite) whereas djurleite which has x in the range from 1.935 to 1.955, E_{gdir} takes the value 1.3 eV (Nair et al., 1998). The electrical conductivity of the material also varies with composition from 0.07 to 2400 $ohm^{-1}\,cm^{-1}$ when x varies from 2 to 1.8 (Nair et al., 1998). The Cu_xS thin films are effectively used in

* Corresponding author. Tel.: +91 824 2474 3608; fax: +91 824 2474 4033.
E-mail address: snoelvictoria@gmail.com (S. Noyel Victoria).
Peer review under responsibility of King Saud University.

ELSEVIER Production and hosting by Elsevier

http://dx.doi.org/10.1016/j.arabjc.2015.03.013

solid junction solar cells which have many applications as it is a direct energy conversion device (Sartale and Lokhande, 2000). The short-circuit current (I_{sc}) of a heterojunction solar cell using Cu_xS as absorber layer solar cell is dependent on the value of x. It was observed that with increase in the value of x, short-circuit current increases (Sartale and Lokhande, 2000). The Cu_xS thin films have been found to have near ideal solar control features with the transmittance in the infrared $<10\%$ and high reflectivity in the near infrared region (Isac et al., 2007).

There are reports on various stoichiometric copper sulphide nanoparticles synthesis by high temperature solution phase methods (Ye and Qi, 2008), low temperature solution route (Ye and Qi, 2008), colloidal route (Boey et al., 2007), microemulsion method (Solanki et al., 2010), sonochemical route (Kumar et al., 2002; Wang et al., 2002), thermolysis route (Larsen et al., 2003), microwave assisted heating (Liao et al., 2003), solvothermal route (Gorai et al., 2005a; Gorai et al., 2005b), chemical precipitation route (Pop et al., 2011), electrophoresis deposition (Sabet et al., 2014) and successive ionic layer adsorption and reaction (SILAR) method (Sartale and Lokhande, 2000). However, the solvothermal route requires high pressure and temperature conditions, thermal routes need high temperature conditions and liquid phase synthesis at low temperature involves more reaction time. Microwave method and sonochemical synthesis share an advantage of reduced reaction time. The $CuInS_2$ and CuS nanoparticles were reported to be synthesized by microwave method (Sabet et al., 2011; Sabet et al., 2012; Sabet et al., 2013; Yousefi et al., 2012a). Apart from $CuInS_2$, various solar cell materials have also been synthesized and used microwave method (Yousefi et al., 2012b). The use of ultrasonic waves for the nanoparticle synthesis has been in practice for many decades. Many metal and metal oxide nanoparticles have been successfully synthesized using sonochemical method (Xu et al., 2003; Xu et al., 2013). Apart from these, the semiconductor nanomaterials have also been synthesized using sonochemical methods (Gao et al., 2005; Xu et al., 2003; Xu et al., 2013; Amiri et al., 2013; Amiri et al., 2014). Among the solar cell materials, $CuInS_2$ has been synthesized by sonochemical route (Amiri et al., 2013; Amiri et al., 2014). The ultrasonic irradiation helps in refining the shape of the desired particle, changes the surface morphology and also helps in degassing of the medium (Chu et al., 2006). The most dominant effects of ultrasonic waves are cavitation and acoustic streaming. The collapse of the bubbles causes hot spots with transient temperatures of 5000 K and cooling rates in excess of 10^{10} K s^{-1}. These extreme conditions during sonication cause enhanced mixing, which helps in decreasing the particle size and increasing the reactive surface area (Gao et al., 2005; Xu et al., 2003; Xu et al., 2013). There is relatively less report on the sonochemical synthesis of copper sulphides (Xu et al., 2003; Xu et al., 2013).

The present work reports the single step sonochemical synthesis of copper sulphide nanoparticles under various reaction conditions. The morphology of particles was studied by scanning electron microscopy (SEM) and transmission electron microscopy (TEM). The crystal nature of the particles was analysed by X-ray diffraction (XRD). The optical properties were studied using UV–visible spectroscopy (UV–vis).

2. Experimental

2.1. Material

Copper sulphide nanoparticles were synthesized using liquid phase synthesis method in the presence of ultrasonic irradiation. Copper acetate monohydrate (99%), thiourea (99%) and NaOH (99%) were used as the precursor materials for the synthesis. All the chemicals used were of analytical grade. Deionized water was used for all the experiments. A 200 mM copper acetate solution was used as copper precursor. Thiourea solution of 1.8 M was used as sulphur precursor. The pH of the thiourea precursor solution was 13.4.

2.2. Synthesis

Bath type ultrasonicator (Elmasonic P60H) was used for the synthesis of the Cu_xS nanoparticles. To the copper precursor solution in the ultrasonic bath, the sulphur precursor solution was added dropwise. The solution pH tends to drop with progress of reaction; however, it was maintained at pH 5.5 by adding NaOH. The temperature of the ultrasonic bath was maintained constant by circulating the cold water. Black precipitate formed was centrifuged and washed with acetone and distilled water at least ten times to remove the impurities. All the synthesis experiments were conducted at 37 kHz frequency. The experiment was performed at different bath temperatures and sonication times. The powder thus obtained was heated at various temperatures to study the effect of treatment temperatures.

2.3. Characterization

The crystallinity of the synthesized samples was characterized by XRD (PANalytical 3 kW X'pert Powder XRD), surface morphology was studied using scanning electron microscope (JEOL) and composition was analysed using EDX station (JED-2300). The particle size was characterized using transmission electron microscopy unit (TEM, JEOL 3010). The optical characterization studies were done in UV–visible spectrophotometer (Labomed UVD-3500). The thermal characterization was performed in a Perkin Elmer thermal analyzer. For electrical characterization, the Cu_xS sample was dispersed in water and filtered to get a thick residue, which was coated on an Indium coated tin oxide (ITO) substrate (Sigma Aldrich, 25 Ω) using doctor blade technique. The coating thickness for the samples varied between 4 μm and 5 μm. To the coated slide another ITO coated glass slide was placed and IV characterization studies were made. The IV studies were conducted in a CHI660E (CH instruments, USA) electrochemical workstation. The linear sweep voltammetry was carried out with a scan rate of 0.1 V s^{-1} in a potential range ±1 V.

3. Results and discussion

3.1. X-ray diffraction

The results of the XRD analysis for the samples synthesized at different bath temperatures, different sonication times and

Please cite this article in press as: Singh, A. et al., Simple one-pot sonochemical synthesis of copper sulphide nanoparticles for solar cell applications. Arabian Journal of Chemistry (2015), http://dx.doi.org/10.1016/j.arabjc.2015.03.013

different calcination temperatures are shown in Fig. 1. The XRD results in all the cases show high intensity peaks at 2θ values of 31.7° and 32.7° which corresponds to $Cu_{1.92}S$ and tetragonal $Cu_{1.81}S$, in accordance with the JCPDS 30-0505 and 41-0959 respectively (Andronic et al., 2011; Ye et al., 2014). The medium intensity peaks at 37.2°, 42.5°, 44.8°, 48.3° and 51.5° show the presence of hexagonal Cu_2S (JCPDS-26-1116) with lattice constant $a = 3.9610$ A, $b = 3.9610$ A and $c = 6.7220$ A (Head, 2009). The peaks at 33.8° and 35.2° show the presence of $Cu_{1.97}S$, orthorhombic djurleite (JCPDS-20-0365). In fact, these peaks also match with chalcocite phase (JCPDS-31-0482). Peaks at 42°, 50° and 56° correspond to rhombohedral digenite, $Cu_{1.8}S$ (JCPDS 26-0476 and 47-1748) with $a = 3.951$ and $c = 48.13$ A (Ramirez et al., 2014; Kumar et al., 2012). The particles synthesized at 55 °C show decreased intensity and broadening of the peaks with increase in sonication time. A decrease in the intensity of the peaks with broadening of the peaks indicates decreased crystallinity and decrease in size of the particles (Vasuhi et al., 2014). The amorphous nature increases with the sonication time (Vasuhi et al., 2014). The particles synthesized with 60 min sonication time at different bath temperatures also showed decreased crystallinity with increase in bath temperature. The heat treatment of the sample synthesized at 45 °C bath temperatures with 60 min sonication time also showed similar trend of decreased crystallinity with increase in treatment temperature. Decreased crystallinity with sonication treatment time was also observed in the case of cellulose and chitosan (Sumari et al., 2013; Yuliana et al., 2012).

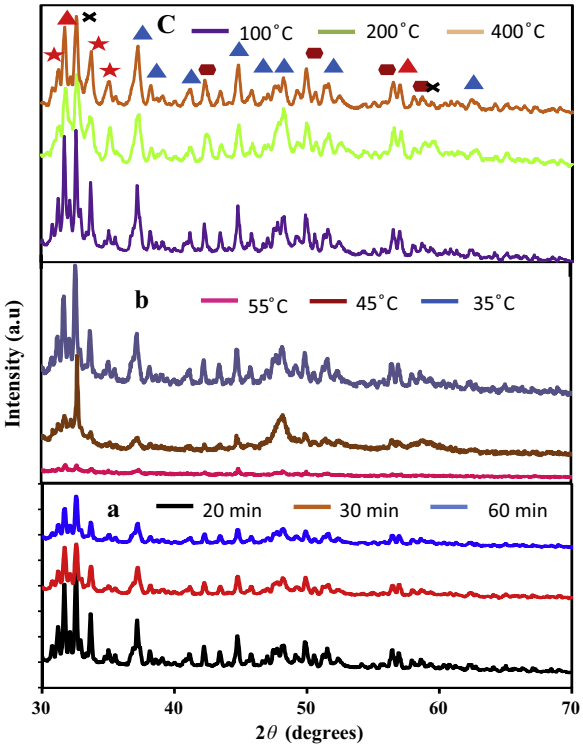

Figure 1 XRD patterns of copper sulphide particles synthesized at different conditions. a. sonication time, b. sonication temperature and c. annealing temperature (★ – $Cu_{1.98}S$, ▲ – Cu_2S, ▲ – $Cu_{1.92}S$, ✕ – $Cu_{1.81}S$, ● – $Cu_{1.8}S$).

It is also shown that increase in the sonication bath temperature along with increased sonication time resulted in decreased crystallinity (Yuliana et al., 2012). The deceased crystallinity with increase in the sonication time could be due the formation of hot spots during the collapse of cavitation and physical stress due to the acoustic cavitation (Sumari et al., 2013). The loss of crystallinity during heating could be due to liberation of gases during transformation of CuS to other forms (Yousefi et al., 2012b).

The crystallite size of the particles under various reaction conditions was calculated using Debye–Scherrer equation (Eq. (1)) (Vasuhi et al., 2014):

$$t = \frac{K\lambda}{\beta cos\theta} \quad (1)$$

where t is crystallite size, K is a crystallite shape factor which takes the value of 0.9, λ is the wavelength of X-ray which is 0.154 nm for Cu Kα, β is full width at half maximum (FWHM) in radians and θ is the Bragg's diffraction angle. The crystallite sizes thus calculated are presented in Table 1. The crystallite size decreases with increase in sonication time for the samples synthesized while maintaining the bath temperature at 35 °C. The crystallite size of the particles was found to increase for the particles synthesized at different bath temperatures with 60 min sonication time. However, the crystallinity is lost completely at an ultrasonic bath temperature of 55 °C. The particles synthesized at 45 °C bath temperatures with 60 min sonication time showed an increase in crystallite size at 100 °C and 200 °C but decreased for heat treatment at 400 °C.

3.2. UV–vis spectroscopy

The absorbance characteristics of the samples synthesized under different sonication times at 35 °C bath temperature are shown in Fig. 2. All the particles show a broad absorption peak over the entire visible region. The broad absorption peak over the entire visible region is a desirable feature for solar cell window material. The absorbance pattern also shows absorbance in the near infrared region towards visible range, which makes it ideal for solar cell application (Vasuhi et al., 2014). A sharp increase in the absorbance in the wavelength range 500 nm matches with the earlier reports and it is close to the effective band gap of Cu_2S (Vasuhi et al., 2014). The band

Table 1 Crystal size and band gap of copper sulphide synthesized at different conditions.

Sonication time (min)	Ultrasonic bath temperature (°C)	Heat treatment temperature (°C)	Crystal size (Å)	Band gap (eV)
20	35	Air dried	28.11	1.75
30	35	Air dried	27.42	1.8
60	35	Air dried	25.58	1.8
60	45	Air dried	29.13	2
60	55	Air dried	39.61	2.1
60	45	100	35.16	1.3
60	45	200	40.76	1.5
60	45	400	34.50	1.6

gap of the synthesized particles was calculated using the Tauc relation (Eq. (2)) (Mehta et al., 2009):

$$\varepsilon h\upsilon = A(h\upsilon - E_g)^n \quad (2)$$

where ε is the molar extinction coefficient, A is a constant, E_g is optical band gap of the sample and $h\upsilon$ is photon energy. In Eq. (2), n depends on type of transition which is ½ and 2 for direct and indirect allowed transitions respectively. The $(\varepsilon h\upsilon)^2$ values are plotted with $h\upsilon$ values, and the intersection of the slope to curve at x axis gives the optical band gap of the synthesized Cu_xS nanoparticles. The Tauc plots for all the samples are shown in Fig. 3. The band gap values calculated from the Tauc plots are shown in Table 1. It is clear from Table 1 that the optical band gap of the particles slightly increases from 1.75 eV to 1.8 eV with increase in sonication time at a constant bath temperature of 35 °C. The crystallite size increases with increase in the bath temperature at a constant sonication time of 60 min. Generally the band gap should decrease for larger sized particles. However, from Table 1, it is seen that with increase in the size of the particles the band gap increases. The XRD studies reveal that the amorphous nature of the particles increases with increase in sonication bath temperature. The band gap of the amorphous particles is reported to be higher when compared to their crystalline counterparts. The increased degree of disorder in amorphous particles results in decreased absorbance leading to higher band gap energy (Rotaru et al., 1999). The optical band gap of the particles heated at 100 °C is 1.3 eV whereas for the particles heated at 400 °C the band gap increased significantly to 1.6 eV which can also be explained by the loss of crystallinity and accompanying phase transformation. The transmittance spectra for the particles synthesized at various conditions are shown in Fig. 4. The transmittance spectra for the particles synthesized under different sonication times show decreased transmittance values with time. However, they show an increasing trend in the transmittance values in the lower wavelength region and decreasing trend in the higher wavelength range. This phenomenon is reported earlier when Cu_2S was deposited using chemical bath deposition (Vasuhi et al., 2014). The increase in transmittance in the shorter wavelength region is attributed to the inter-band transitions from valence band towards the conduction band. The decrease in transmittance in the higher wavelength zone is due to the increase in carrier concentration (Vasuhi et al., 2014). Particles synthesized under different bath temperatures also showed similar trend. The samples annealed at 400 °C showed higher transmittance value in all the wavelengths. The heat treatment was found to increase the optical transmittance values in all three calcination temperatures. All the particles synthesized under various conditions show maximum absorbance in the wavelength range from 630 nm to 680 nm. The transmittance values in all the cases are above 50% which makes them an ideal candidate for solar control coatings (Vasuhi et al., 2014).

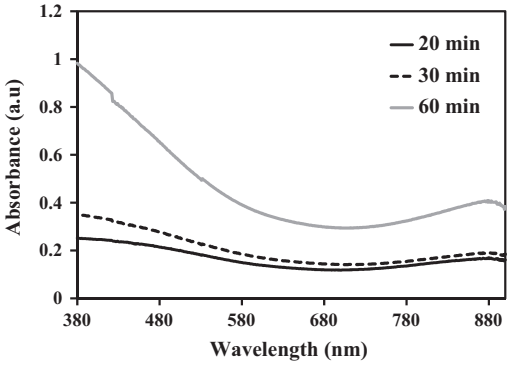

Figure 2 Absorbance spectra of copper sulphide particles synthesized at different sonication time.

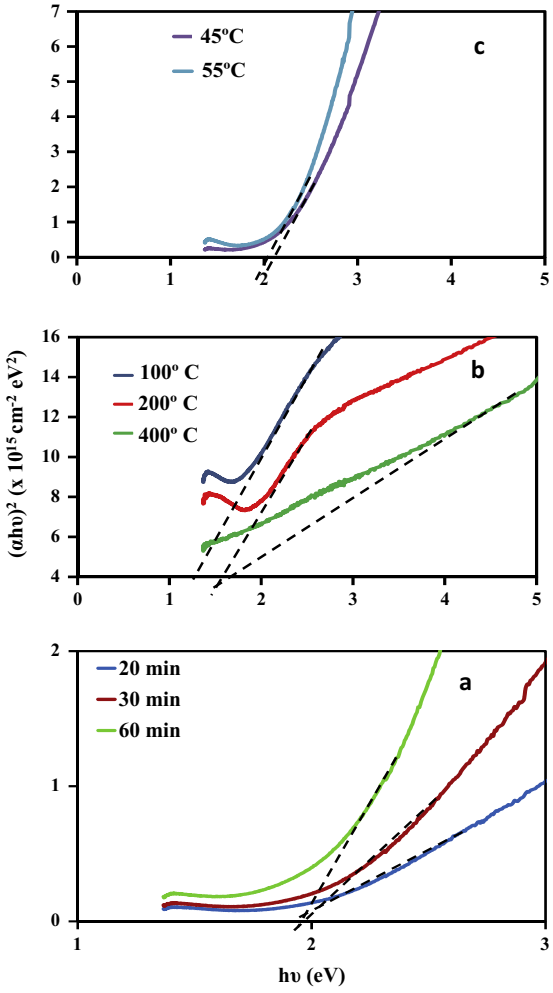

Figure 3 Tauc plot for copper sulphide particles synthesized at different conditions. (a) Sonication time, (b) annealing temperature and (c) sonication temperature.

3.3. Scanning electron microscopy (SEM) and transmission electron microscopy (TEM)

Fig. 5(a)–(d) shows SEM images of the Cu_xS particles synthesized at various reaction conditions. The scanning electron microscopy (SEM) results show that the size of the particles reduces with sonication time. The particles synthesized at 45 °C bath temperature with 60 min sonication time show relatively low polydispersity. The particles synthesized at 55 °C bath temperature and 60 min sonication time show the presence of few nanoplates. The particle size increases with the temperature of the sonication bath. The XRD analyses also show that the crystallite size increases with increase in

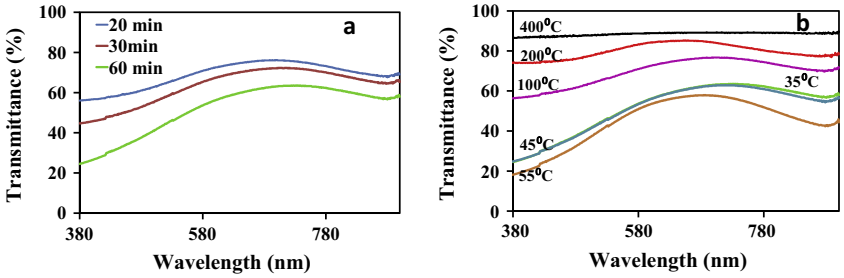

Figure 4 Transmittance spectra of the copper sulphide particles synthesized at different conditions. (a) Sonication time and (b) sonication temperature and annealing temperature.

sonication bath temperature. Sonication at higher temperatures has been linked to the formation of larger sized particles due to agglomeration or reducing intensity of collapse due to the cushioning effect of the increasing cavity vapour pressure at higher temperatures (Ambedkar, 2012). The formation of nanoplates at 55 °C could be attributed to the above-mentioned effects. Particles synthesized at 45 °C with 60 min sonication time, when calcined at 400 °C showed the formation of needle like nanorods. These could be due to the transformation of CuS to other forms during heat treatment. Such morphological changes due to transformation are confirmed from the earlier work which reported the formation of tetragonal $Cu_{1.81}S$ from $Cu_{1.9}S$ resulted in the change in morphology from nanospheres to nanorods (Li et al., 2014; Yousefi et al., 2012b). The TEM images of the particles synthesized at 45 °C with 1 h sonication time are shown in Fig. 6. It is seen from Fig. 6-a, that most of the particles are spherical with few nanorods. The size of the particles is in the range of 15–20 nm. The lattice spacing of the particle shown in Fig. 6b was found to be 0.19 nm which corresponds to the monoclinic $Cu_{1.8}S$ (Tiong et al., 2014). The lattice spacing of the particle in Fig. 6c is 0.33 nm, which corresponds to Cu_2S (Ding et al., 2012) as in Fig. 6c. The SAED measurements confirmed that the particles are crystallized and the diffraction pattern matches with the XRD peaks well, as seen in Fig. 6d.

3.4. IV Characterization

Fig. 7a–c shows the current voltage characteristics of ITO/Cu_xS/ITO structures in the presence and absence of 200 W light source which was kept at a height of 55 cm from the sample. The Cu_xS synthesized at different sonication bath temperatures were used to form coating. Fig. 8a–c shows the IV curves of the samples heated at different temperatures. In all the cases, the IV curves show linear behaviour which suggests the ohmic nature of the Cu_xS. The resistance for the samples synthesized at different sonication bath temperatures is 0.03 Ω cm^{-2} and for the heat treated samples is 0.05 Ω cm^{-2}. The IV studies show that the coating is conductive with minimum resistance.

3.5. Thermal characterization

Fig. 9 shows the results of the thermogravimetric analysis (TGA) of the CuS nanoparticles synthesized at 35 °C bath

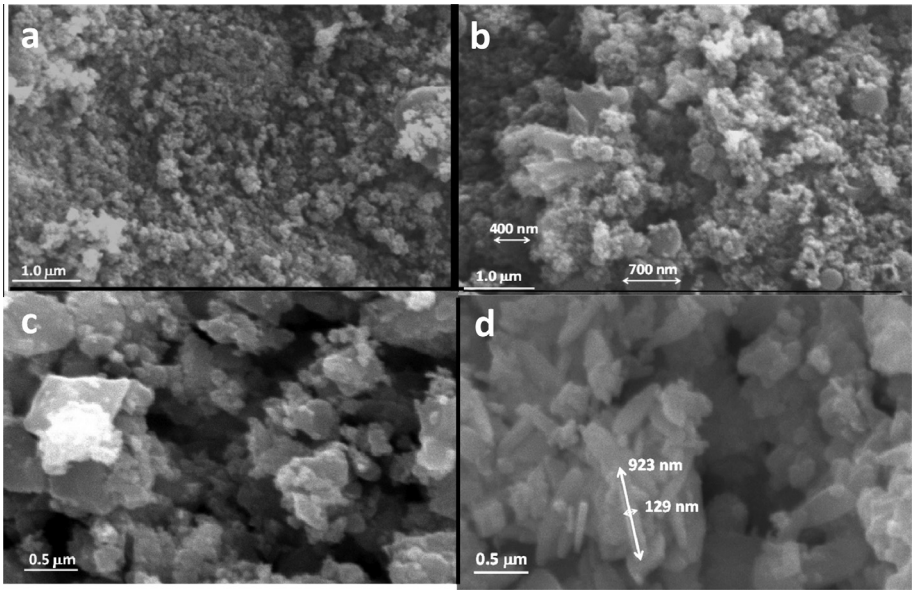

Figure 5 SEM images of copper sulphide particles synthesized at different sonication temperature. (a) 45 °C bath temperature 1 h sonication time, (b) 55 °C bath temperature 1 h sonication time, (c) 45 °C synthesized particle at 100 °C calcination and (d) 45 °C synthesized particle at 400 °C calcination.

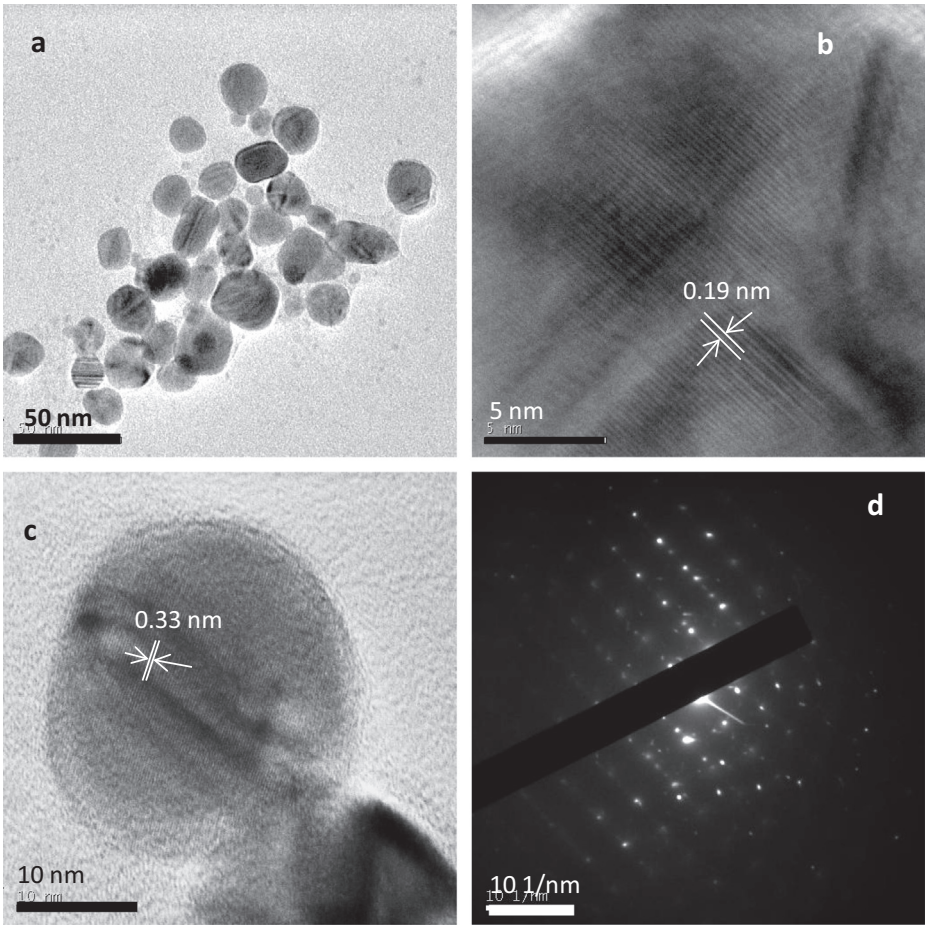

Figure 6 TEM images of copper sulphide particles synthesized at sonication time of 60 min at 45 °C and air dried (without annealing). (a) TEM image showing the morphology, (b) TEM image showing the lattice spacing of 0.19 nm – monoclinic $Cu_{1.8}S$, (c) TEM image showing the lattice spacing of 0.33 nm – Cu_2S and (d) SAED pattern of synthesized particle.

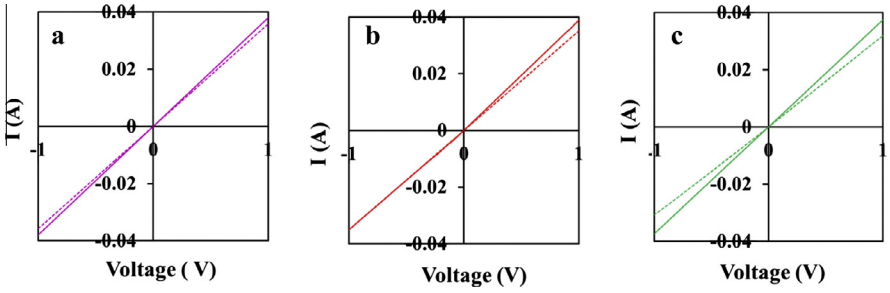

Figure 7 IV characteristic curves of ITO/Cu_xS/ITO with the Cu_xS synthesized at various sonication bath temperatures. (a) 35 °C, (b) 45 °C, (c) 55 °C. The solid line represents IV curves in the presence of 200 W light source and the dotted lines represent dark.

temperature with 60 min sonication time. The TGA was conducted in the oxygen environment from 50 °C to 700 °C with a heating rate of 15 °C min^{-1}. Fig. 10 shows the differential scanning calorimetry (DSC) results for the same sample from room temperature to 350 °C. The thermogram shows weight loss of approximately 42% with various decomposition stages. It was shown by the earlier studies that the CuS decomposition in air follows many steps with various forms of copper sulphides ($Cu_{1.8}S$, Cu_2S), copper oxides (Cu_2O, CuO), copper sulphates (Cu_2SO_4, $CuSO_4$), and copper oxy-sulphates as products (Nafees et al., 2013). In general, the increase in mass is attributed to the formation of sulphates and loss of mass is believed to be associated with oxidation, release of sulphur dioxide and evaporation of water (Dunn and Muzenda, 2001). The DSC studies show endothermic peaks at 100 °C, 123 °C and at 225 °C. The endothermic peak at 100 °C and

Please cite this article in press as: Singh, A. et al., Simple one-pot sonochemical synthesis of copper sulphide nanoparticles for solar cell applications. Arabian Journal of Chemistry (2015), http://dx.doi.org/10.1016/j.arabjc.2015.03.013

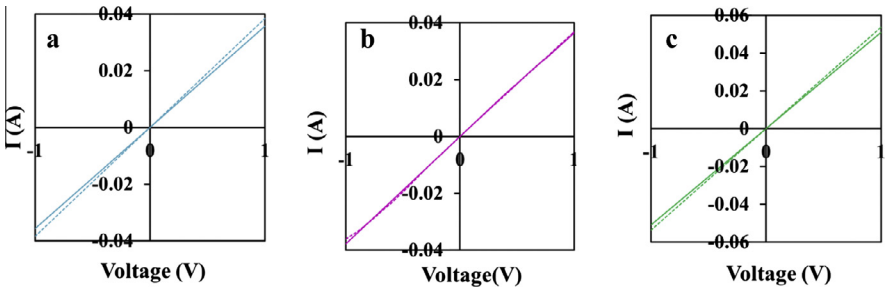

Figure 8 IV characteristic curves of ITO/Cu_xS/ITO with the Cu_xS synthesized at various heat treatment temperatures. (a) 400 °C, (b) 200 °C and (c) 100 °C. The solid line represents IV curves in the presence of 200 W light source and the dotted lines represent dark.

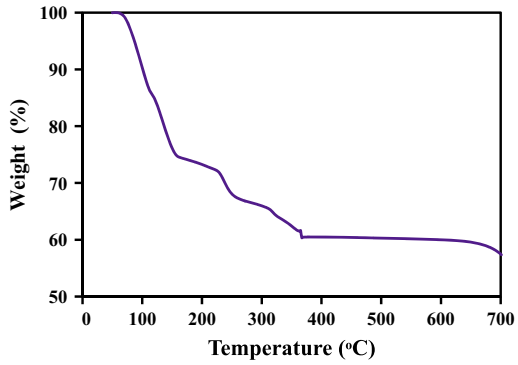

Figure 9 Thermogram of Cu_xS particles synthesized at 35 °C bath temperature with 1 h sonication time (in the oxygen environment).

123 °C and the corresponding weight loss could be due to the evaporation of water (Simonescu et al., 2007). The peak at 225 °C may be due to the transformation of CuS to cubic digenite (Nafees et al., 2013; Simonescu et al., 2007; Dunn and Muzenda, 2001). This initial reaction in the temperature range from 220 °C to 260 °C is given by

$$1.8CuS + 0.8O_2 \rightarrow Cu_{1.8}S + 0.8SO_2 \quad (3)$$

A second reaction occurs between 300 °C and 370 °C resulting in the formation of Cu_2S (Dunn and Muzenda, 2001) which corresponds to the weight loss in that temperature interval. No significant weight loss was observed from 400 °C to 700 °C.

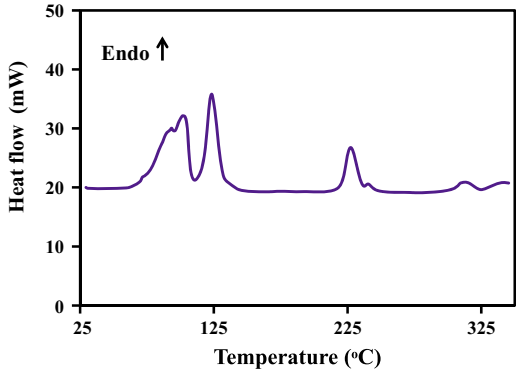

Figure 10 DSC of Cu_xS particles synthesized at 35 °C bath temperature with 1 h sonication time.

$$2CuS + O_2 \rightarrow Cu_2S + SO_2 \quad (4)$$

3.6. Mechanism

The reaction was conducted in alkaline medium. The use of copper acetate monohydrate leads to the reduction in pH with the progress of the reaction, which was adjusted by addition of excess NaOH. The series of reactions involved in the formation of Cu_xS are given below:

$$H_2O \;))))) \; H^{\cdot} + OH^{\cdot} \quad (5)$$

$$H_2NCSNH_2 + 2OH^{\cdot} \rightarrow 2NH_3 + CO_2 + S^{2-} \quad (6)$$

$$S^{2-} + S^{2-} \rightarrow (S \ldots S)^{3-} \rightarrow (S \ldots S)^{2-} \quad (7)$$

$$x\text{Cu(II or I)} + S^{2-}(\text{or } S_2^{2-}) \rightarrow Cu_xS \quad (8)$$

In an aqueous sonochemical process, the pyrolysis of water occurs due to the elevated temperature and pressure conditions inside the collapsing bubble (Wang et al., 2002). The possible products of the water pyrolysis reaction are shown in Eq. (5) (Sheng et al., 2008). The thiourea undergoes hydrolysis reaction resulting in the production of S^{2-} ions (Eq. (6)) (Sheng et al., 2008). The reaction is also accompanied by reduction of Cu(II) to Cu(I), which changes the colour of the precursor solution from blue to aqua (Sheng et al., 2008). The formation of Cu_xS particles is given by the Eq. (8) (Sheng et al., 2008).

4. Conclusion

An attempt to synthesize Cu_xS by sonochemical route was made. The synthesized particles were mixture of $Cu_{1.8}S$, Cu_2S and $Cu_{1.97}S$. The band gap of the particles was in the range of 1.3–2.1 eV. The crystallite size and composition were found to influence the optical band gap. Spherical shaped particles and nanorods were formed at 45 °C bath temperature with 1 h sonication time. Particles synthesized at 55 °C bath temperature with 1 h sonication time showed the presence of nanoplates and the particles synthesized at 45 °C with 1 h sonication time upon calcination at 400 °C showed the presence of needle like nanocrystals. The TGA shows that the heat treatment causes the formation of amorphous product due to evaporation of water and sulphur dioxide formation and transformation of CuS to other forms. The IV characterization shows that the deposit exhibits ohmic nature with a resistance in the range 0.03 Ω cm^{-2} to 0.05 Ω cm^{-2}.

References

Ambedkar, B., 2012. Ultrasonic Coal-wash for De-ashing and De-sulfurization Experimental Investigation and Mechanistic Modeling. Springer-Verlag, Berlin Heidelberg.

Amiri, O., Salavati-Niasari, M., Sabet, M., Ghanbari, D., 2013. Synthesis and characterization of CuInS2 microsphere under controlled reaction conditions and its application in low-cost solar cells. Mater. Sci. Semicond. Process. 16, 1485–1494.

Amiri, O., Salavati-Niasari, M., Sabet, M., Ghanbari, D., 2014. Sonochemical method for preparation of copper indium sulfide nanoparticles and their application for solar cell. Comb. Chem. High Throughput Screening 17, 183–189.

Andronic, L., Isac, L., Duta, A., 2011. Photochemical synthesis of copper sulphide/titanium oxide photocatalyst. J. Photochem. Photobiol., A 221, 30–37.

Boey, H.T., Tan, W.L., Bakar, N.H.H.A., Bakar, M.A., Ismail, J., 2007. Formation and morphology of colloidal chitosan-stabilized copper sulfides. J. Phys. Sci. 18, 87–101.

Chu, S.-H., Choi, S.-H., Kim, J.-W., King, G.C., Elliott, J.R., 2006. Ultrasonication of bismuth telluride nanocrystals fabricated by solvothermal method. Proc. SPIE 61720A.

Ding, X., Zou, Y., Jiang, J., 2012. Au–Cu_2S heterodimer formation *via* oxidation of AuCu alloy nanoparticles and *in situ* formed copper thiolate. J. Mater. Chem. 22, 23169–23174.

Dunn, J.G., Muzenda, C., 2001. Quantitative analysis of phases formed during the oxidation of covellite (CuS). J. Therm. Anal. Calorim. 64, 1241–1246.

Gao, T., Li, Q., Wang, T., 2005. Sonochemical synthesis, optical properties, and electrical properties of core/shell-type ZnO nanorod/CdS nanoparticle composites. Chem. Mater. 17, 887–892.

Gorai, S., Ganguli, D., Chaudhuri, S., 2005a. Synthesis of flower-like Cu_2S dendrites via solvothermal route. Mater. Lett. 59, 826–828.

Gorai, S., Ganguli, D., Chaudhuri, S., 2005b. Shape selective solvothermal synthesis of copper sulphides: role of ethylenediamine–water solvent system. Mater. Sci. Eng., B 116, 221–225.

Head, J.L.R., 2009. Synthesis and characterization of Cu_xS nanoparticles for solar cell application, Master's Thesis, The University of Arizona.

Isac, L.A., Duta, A., Kriza, A., Enesca, I.A., Nanu, M., 2007. The growth of CuS thin films by spray pyrolysis. J. Phys: Conf. Ser. 61, 477–481.

Kassim, A., Nagalingam, S., Min, H.-S., Karrim, N., 2010. XRD and AFM studies of ZnS thin films produced by electrodeposition method. Arabian J. Chem. 3, 243–249.

Kumar, R.V., Palchik, O., Koltypin, Y., Diamant, Y., Gedanken, A., 2002. Sonochemical synthesis and characterization of Ag_2S/PVA and CuS/PVA nanocomposite. Ultrason. Sonochem. 9, 65–70.

Kumar, P., Gusain, M., Nagarajan, R., 2012. Solvent-mediated room temperature synthesis of highly crystalline Cu_9S_5($Cu_{1.8}S$), CuSe, PbS and PbSe from their elements. Inorg. Chem. 51 (15), 7945–7947.

Larsen, T.H., Sigman, M., Ghezelbash, A., Doty, R.C., Korgel, B.A., 2003. Solventless synthesis of copper sulfide nanorods by thermolysis of a single source thiolate-derived precursor. J. Am. Chem. Soc. 125, 5638–5639.

Liao, X.-H., Chen, N.-Y., Xu, S., Yang, S.-B., Zhu, J.-J., 2003. A microwave assisted heating method for the preparation of copper sulfide nanorods. J. Cryst. Growth 252, 593–598.

Li, X., Tang, A., Guan, L., Ye, H., Hou, Y., Dong, G., Yang, Z., Teng, F., 2014. Effects of alkanethiols chain length on the synthesis of Cu2-xS nanocrystals: phase, morphology, plasmonic properties and electrical conductivity. RSC Adv. 4, 54547–54553.

Mehta, S.K., Kumar, S., Chaudhary, S., Bhasin, K.K., Gradzielski, M., 2009. Evolution of ZnS nanoparticles via facile CTAB aqueous micellar solution route: a study on controlling parameters. Nanoscale Res. Lett. 4, 17–28.

Nafees, M., Ali, S., Idrees, S., Rashid, K., Shafique, M.A., 2013. A simple microwave assists aqueous route to synthesis CuS nanoparticles and further aggregation to spherical shape. Appl. Nanosci. 3, 119–124.

Nair, M.T.S., Guerrero, L., Nair, P.K., 1998. Conversion of chemically deposited CuS thin films to Cu1.8S and Cu1.96S by annealing. Semicond. Sci. Technol. 13, 1164–1168.

Pop, A.E., Batin, M.N., Popescu, V., 2011. The influence of annealing temperature on copper sulphideCu_xS obtained by chemical precipitation. Powder Metall. Progress. 11, 3–4.

Ramirez, P.V., Arenas, M.C., Santos, J., Vega, M., Martínez, O., Meneses, V.M., Torres, L.S., Hernández, J., 2014. Growth evolution and phase transition from chalcocite to digenite in nanocrystalline copper sulfide: morphological, optical and electrical properties. Beilstein J. Nanotechnol. 5, 1542–1552.

Rotaru, C., Nastase, S., Tomozeiu, N., 1999. Amorphous phase influence on the optical bandgap of polysilicon. Phys. Stat. Sol. A 171, 365–370.

Sabet, M., Salavati-Niasari, M., Davar, F., 2011. Facile one-step microwave to prepare $CuInS_2$/CuS nanocomposite for solar cells. Micro Nano Lett. 6 (11), 904–908.

Sabet, M., Salavati-Niasari, M., Ashjari, M., Ghanbari, D., Dadkhah, M., 2012. $CuInS_2$/CuS nanocomposite: synthesis via simple microwave approach and investigation its behavior in solar cell. J. Inorg. Organomet. Polym. 22, 1139–1145.

Sabet, M., Salavati-Niasari, M., Ghanbari, D., Amiri, O., Yousefi, M., 2013. Synthesis of $CuInS_2$ nanoparticles via simple microwave approach and investigation of their behavior in solar cell. Mater. Sci. Semicond. Process. 16, 696–704.

Sabet, M., Salavati-Niasari, Amiri, O., 2014. Using different chemical methods for deposition of CdS on TiO_2 surface and investigation of their influences on the dye-sensitized solar cell performance. Electrochim. Acta 117, 504–520.

Saraf, R., 2012. High efficiency and cost effective Cu_2S/CdS thin-film solar cell. IOSR JEEE 2, 47–51.

Sartale, S.D., Lokhande, C.D., 2000. Growth of copper sulphide thin films by successive ionic layer adsorption and reaction (SILAR) method. Mater. Chem. Phys. 65, 63–67.

Sheng, C.L., Chen, L.D., Yao, Y., Huang, F.Q., 2008. In situ assembly of Cu_xS quantum-dots into thin film: a highly conductive P-type transparent film. J. Phys. Chem. C 112, 12085–12088.

Simonescu, C.M., Teodorescu, V.S., Carp, O., Patron, L., Capatina, C., 2007. Thermal behaviour of CuS (Covellite) obtained from copper-thiosulfate system. J. Therm. Anal. Calorim. 88 (1), 71–76.

Solanki, J.N., Sengupta, R., Murthy, Z.V.P., 2010. Synthesis of copper sulphide and copper nanoparticles with microemulsion method. Solid State Sci. 12, 1560–1566.

Tiong, V.T., Bell, J., Wang, H., 2014. One-step synthesis of high quality kesterite Cu_2ZnSnS_4 nanocrystals – a hydrothermal approach. Beilstein J. Nanotechnol. 5, 438–446.

Sumari, S., Roesyadi, A., Sumarno, S., 2013. Effects of ultrasound on the morphology, particle size, crystallinity, and crystallite size of cellulose. Sci. Study Res., Chem. Chem. Eng., Biotechnol., Food Ind. 14 (4), 229–239.

Vasuhi, A., Xavier, R.J., Chandramohan, R., Muthukumaran, S., Dhanabalan, K., Ashokkumar, M., Parameswaran, P., 2014. Effect of heat-treatment on the structural and optical properties of Cu_2S thin films deposited by CBD method. J. Mater. Sci.: Mater. Electron. 25, 824–831.

Wang, H., Zhang, J.-R., Zhao, X.-N., Xu, S., Zhu, J.J., 2002. Preparation of copper monosulfide and nickel monosulfide nanoparticles by sonochemical method. Mater. Lett. 55, 253–258.

Xu, C., Zhang, Z., Ye, Q., Liu, X., 2003. Synthesis of copper sulfide nanowhisker via sonochemical way and its characterization. Chem. Lett. 32, 198–199.

Xu, H., Zeiger, B.W., Suslick, K.S., 2013. Sonochemical synthesis of nanomaterials. Chem. Soc. Rev. 42, 2555–2567.

Please cite this article in press as: Singh, A. et al., Simple one-pot sonochemical synthesis of copper sulphide nanoparticles for solar cell applications. Arabian Journal of Chemistry (2015), http://dx.doi.org/10.1016/j.arabjc.2015.03.013

Ye, J., Qi, L., 2008. Solution-phase synthesis of one-dimensional semiconductor nanostructures. J. Mater. Sci. Technol. 24, 529–540.

Ye, H., Tang, A., Yang, C., Li, K., Hou, Y., Teng, F., 2014. Synthesis of $Cu_{2-x}S$ nanocrystals induced by foreign metal ions: phase and morphology transformation and localized surface Plasmon resonance. Cryst. Eng. Commun. 16, 8684–8690.

Yousefi, M., Sabet, M., Salavati-Niasari, M., Hosseinpour-Mashkani, S.M., 2012a. Facile microwave approach for synthesis of copper-indium sulfide nanoparticles and study of their behavior in solar cell. J. Clust. Sci. 23, 491–502.

Yousefi, M., Sabet, M., Salavati-Niasari, M., Emadi, H., 2012b. Synthesis and characterization PbS and Bi2S3 nanostructures via microwave approach and investigation of their behaviors in solar cell. J. Clust. Sci. 23, 511–525.

Yuliana, A., Pradeckta, L.S., Savitri, E., Handaratri, A.R., Sumarno, (2012). The effect of sonication on the characteristics of chitosan. In: Proceeding of International Conference on Chemical and Material Engineering 2012, MSD 14-1-5.

Zhao, Y., Pan, H., Lou, Y., Qiu, X., Zhu, J., Burda, C., 2009. Plasmonic $Cu_{2-x}S$ nanocrystals: optical and structural properties of copper-deficient copper(I) sulphides. J. Am. Chem. Soc. 131, 4253–4261.

Zhao, S., Han, G., Li, M., 2010. Fabrication of copper sulfide microstructures with the bottle- and thorny rod-shape. Mater. Chem. Phys. 120, 431–437.

Please cite this article in press as: Singh, A. et al., Simple one-pot sonochemical synthesis of copper sulphide nanoparticles for solar cell applications. Arabian Journal of Chemistry (2015), http://dx.doi.org/10.1016/j.arabjc.2015.03.013